Semiconductor Physics, Quantum Electronics & Optoelectronics, 2020. V. 23, No 4. P. 385-392.

Physics of microelectronic devices

Fidelity of noisy multiple-control reversible gates

V.G. Deibuk[1*], I.M. Yuriychuk[1], I. Lemberski[2]

[1]*Yuriy Fedkovych Chernivtsi National University, 58012 Chernivtsi, Ukraine*
[2]*International Radio Astronomy Centre, Ventspils University College, Ventspils, Latvia*
[*]*E-mail: v.deibuk@chnu.edu.ua*

Abstract. The effect of frequency noise on correct operation of the multiple-control Toffoli, Fredkin, and Peres gates has been discussed. In the framework of the Ising model, the energy spectrum of a chain of atoms with nuclear spins one-half in a spinless semiconductor matrix has been obtained, and allowed transitions corresponding to the operation algorithm of these gates have been determined. The fidelities of the obtained transitions were studied depending on the number of control qubits and parameters of the radio-frequency control pulses. It has been shown that correct operation of the Toffoli and Fredkin gates does not depend on the number of control qubits, while the Peres gate fidelity decreases significantly with the increasing number of control signals. The calculated ratios of the Larmor frequency to the exchange interaction constant correspond with the results of other studies.

Keywords: quantum computing, multiple-control, Fredkin gate, Toffoli gate, Peres gate, fidelity.

https://doi.org/10.15407/spqeo23.04.385
PACS 03.67.Lx, 61.72.Tt

Manuscript received 20.08.20; revised version received 25.09.20; accepted for publication 28.10.20; published online 19.11.20.

1. Introduction

Development of computer technology is associated with both productivity and miniaturization. These challenges are limited by Moore's law, which is due to the natural constraints on the size of the elementary gates and, from the thermodynamic point of view, lead to an increase in the amount of heat released per unit area of the processor. As a consequence, according to the Landauer principle [1], every lost bit of information is associated with generation of thermal energy, so energy in irreversible circuits is consumed at a logical level. The energy value $kT\ln 2$ (J) per each bit of information losses was experimentally confirmed [2]. The use of reversible logic in information processing and transmission devices makes such devices lossless at both physical and logical levels. The idea of quantum computing, from purely theoretical, is getting practical implementation nowadays [3]. At the atomic level, all processes are reversible, so the idea of creating quantum computers directly relies on the creation and use of reversible digital devices. To this end, many logical reversible gates have been proposed. The most conventionally used for the time being are the three-qubit Toffoli, Fredkin, and Peres gates both in terms of hardware complexity (quantum cost) and experimental implementation capabilities [4-6]. Various schemes have been proposed for their implementation on the basis of elementary one- and two-qubit controlled gates (NOT, CNOT, CV, CV+ *etc.*), which quantum cost is taken to be unity [7]. However, the attempts to build reversible logic circuits that are optimal in terms of the number of primitives (quantum cost) continue. In particular, the quantum cost of the Toffoli and Fredkin gates is known to be 5, and the quantum cost of the Peres gate is 4 [8].

Despite a large number of methods for the synthesis of reversible circuits, their practical implementation depends significantly on the quantum processor manufacturing technologies. Semiconductor quantum processors with a nuclear spin chain in a spinless matrix are a promising version of the NMR quantum computers, due to the large coherence times, relative simplicity in qubit manipulation, and the ability to scale [11, 12]. In this case, the allowed atomic transitions are carried out under action of a sequence of control pulses. Experimental implementation of the simplest three-qubit gates [13] showed that the number of pulses in such a sequence corresponds to the complexity of the computing device. In this case, the number of control pulses is a characteristic of the quantum cost of the circuit, and these quantities are not always consistent with each other. An important challenge in building a scalable quantum computer on the base of a spin qubits chain is an accuracy of the implementation of the reversible lossless quantum gates. In particular, it is an optimal choice of quantum elements of the reversible logic, both in terms of their physical implementation and functional versatility. In our opinion, such gates may be the multiple-control Toffoli, Fredkin, and Peres ones. In addition, these gates are important components of the quantum error correction schemes [1]. The practical implementation of the reversible quantum gates can also be estimated by the fidelity of operations [5], caused by various technological factors (an inaccuracy in tuning of the magnetic fields by their amplitude and frequency, number of control pulses, nature of interaction between qubits) and decoherence, which, in particular, can lead to broadening the system energy levels, *etc*.

In the paper, we discuss implementation of the multiple-control Toffoli, Fredkin and Peres gates in the model of a nuclear spin chain in a spinless semiconductor matrix. Comparison of the number of the required transitions, which realizes correct operation of the gate, with the number of control qubits has been performed. It has been shown that the complexity of the multiple-control Toffoli, Fredkin gates in this technical implementation does not depend on the number of control qubits. The number of π-pulses (quantum cost) providing correct operation of the different multiple-control gates has been discussed. The main purpose of the paper was to study the effect of noise on correct operation of the multiple-control gates. In particular, the effect of the frequency imbalance on the fidelity of these gates is considered. The effect of exchange interaction between the qubits for improving the correctness of the gate operation has been also studied.

2. Preliminaries

2.1. Physical model and its implementation

To describe the gates and the effect of noise on them, their technical parameters in the presence of noise, we consider the one-dimensional Ising spin model for a system of N interacting nuclear spins one-half, which are linearly spaced along the x-axis as the quantum-mechanical physical model of the quantum processor. This simple model allows one to analyze and evaluate processes in the gates to be considered. The chain of spins is under action of a strong magnetic field directed along the z-axis and a control transverse radio-frequency (RF) field with a circular polarization in the (xOy) plane.

Physical implementation of the gates based on semiconductor nanotechnology is associated with the ability to control the nuclear spin states of the impurity atoms (qubits) in a semiconductor spinless matrix [4]. We call as allowed the transition between the energy levels of this system, if it satisfies the Pauli principle (change in only one spin state), what implies changing an output state. We consider both pure (digital) and superposition states. For example, the uniformly filled superposition state for four-qubit system can be represented as

$$\frac{1}{\sqrt{16}}\left(|0000\rangle + |0001\rangle + \ldots + |1111\rangle\right).$$

2.2. Gates structure

The three-qubit Toffoli gate consists of two control inputs, which are transmitted directly to the output, and one information input signal, which is added by modulo two to the product of the control signals and appears at the output (Control-Control-NOT). Generalized N-qubit ($N > 3$) Toffoli gate (Fig. 1) can be described as follows:

$$Y_i = X_i\,, 1 \le i \le N-1,$$
$$Y_N = X_1 X_2 \ldots_{N-1} \oplus X_N\ , \tag{1}$$

where X_i and $Y_i = X_i$ ($i = 1, \ldots, N-1$) are the input and output control qubits respectively, and X_N and Y_N are the input and output controlled qubits.

The Fredkin gate also has three input qubits, one of which is control and is transmitted to the output without changing. Two other input lines, depending on the number of control qubits, can exchange information with each other or transmit to the output without changes (Control-SWAP). For the generalized Fredkin gate (Fig. 1), the output and input signals are related as follows [9]:

$$Y_i = X_i\,, 1 \le i \le N-2,$$
$$Y_{N-1} = X_{N-1}\overline{X_1 X_2 \ldots X_{N-2}} \oplus X_N X_1 X_2 \ldots X_{N-2}\,,$$
$$Y_N = X_N \overline{X_1 X_2 \ldots X_{N-2}} \oplus X_{N-1} X_1 X_2 \ldots X_{N-2}\,. \tag{2}$$

Along with the functional completeness of the Fredkin gate, unlike the Toffoli gate, it is parity-preserving, that is, the sum by modulo two of the inputs signals is equal to the sum of the output signals, which is an important advantage.

The three-qubit Peres gate has a minimum quantum cost (QC = 4) among all three-qubit gates. Its multiple-controlled generalizations were proposed in [10], and can be described as follows:

$$Y_i = \bigoplus_{j=1}^{i} X_j \quad i = 1, \ldots, N-1\,,$$
$$Y_N = X_N \oplus X_1 X_2 \ldots X_{N-1}\,. \tag{3}$$

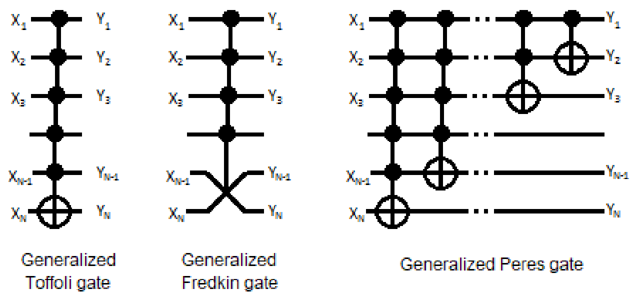

Fig. 1. Generalized N-qubit Toffoli, Fredkin, and Peres gates.

3. System spectrum and dynamics

The full energy operator corresponding to the Hamiltonian of the system can be written in the form:

$$\hat{H} = \hat{H}_0 + \hat{W}\,, \tag{4}$$

where

$$\hat{H}_0 = -\hbar\left(\sum_{k=0}^{N-1}\omega_k I_k^z + 2J\sum_{k=0}^{N-2} I_k^z I_{k+1}^z + 2J'\sum_{k=0}^{N-3} I_k^z I_{k+2}^z\right), \tag{5}$$

$$\hat{W} = -\frac{\hbar\Omega}{2}\sum_{k=0}^{N-1}\left[I_k^+ \exp(i\omega t) + I_k^- \exp(-i\omega t)\right]. \tag{6}$$

Here, we use the following notations: I_k^z is the spin projection operator of the k-th nucleus on the z-axis; $\omega_k = \gamma B(x_k)$ – Larmor frequency; γ – proton gyromagnetic ratio; J and J' are the coupling constants between the nearest and second-nearest neighbors exchange interactions. The magnetic field is taken into account as $\boldsymbol{B}$ = ($b\cos\omega t$, $-b\sin\omega t$, $B(x_k)$); $\Omega = \gamma b$ is the Rabi frequency corresponding to a transverse field with the amplitude b. This controlling RF field is used to control the direction of the spin and can be considered as a perturbation, since it is much smaller than the static magnetic field $B(x_k)$. The process of spin tuning can be described by the ascent and descent operators $I_k^+ = |0_k\rangle\langle 1_k|$ and $I_k^- = |1_k\rangle\langle 0_k|$ for the k-th spin.

Solving the stationary Schrödinger equation on the basis of the nuclear spins eigenstates $|i_{N-1},...,i_2,i_1,i_0\rangle$, one can obtain the energy spectrum of the (2^N) spin system. The values of i_N are equal to 0 or 1 and represent the content of each digit, depending on the spin orientation of each qubit. Operation algorithm of the logical element is provided by the transitions between the obtained energy levels under action of the external controlling field with the frequency ω. Time evolution of the system can be described by the non-stationary, *i.e.* time-dependent, Schrödinger equation:

$$i\hbar\frac{\partial\Psi(t)}{\partial t} = \hat{H}\Psi(t). \tag{7}$$

The complete wave function $\Psi(t)$ can be presented in the full basis $|i_{N-1},...,i_2,i_1,i_0\rangle$. The details of finding a numerical solution of (7) can be found in [14].

Implantation of the ^{31}P ions with $|\uparrow\rangle$ and $|\downarrow\rangle$ nuclear spins states into a spinless isotope-enriched ^{28}Si semiconductor matrix revealed that these spin qubits have a record-breaking decoherence time exceeding 30 seconds, and fidelities of the single-qubit gates reach 99% [4]. This intriguing fact stipulates a modeling of more complex reversible fault-tolerant multiple-control gates on the base of the above mentioned simple model. In particular, the following parameters were selected: the Larmor frequencies of the qubits varied as $\omega_k = 100\cdot 2^k$, (k = 0, 1, …, $N-1$). This is achieved by changing the magnitude of the magnetic field $B(x_k)$ gradient along the x-axis. The parameters of the exchange interaction J and J' between the first and second neighbors were chosen to satisfy the condition of the selective excitation ($\Omega \ll J \ll \omega$). The stationary energy levels for the multiple-control Toffoli, Fredkin, and Peres gates (Fig. 2) are found from the solution of the stationary Schrödinger equation for the Hamiltonian of the non-perturbed system (5). In the calculations, the first qubits are considered as control, and the last qubits as the target ones.

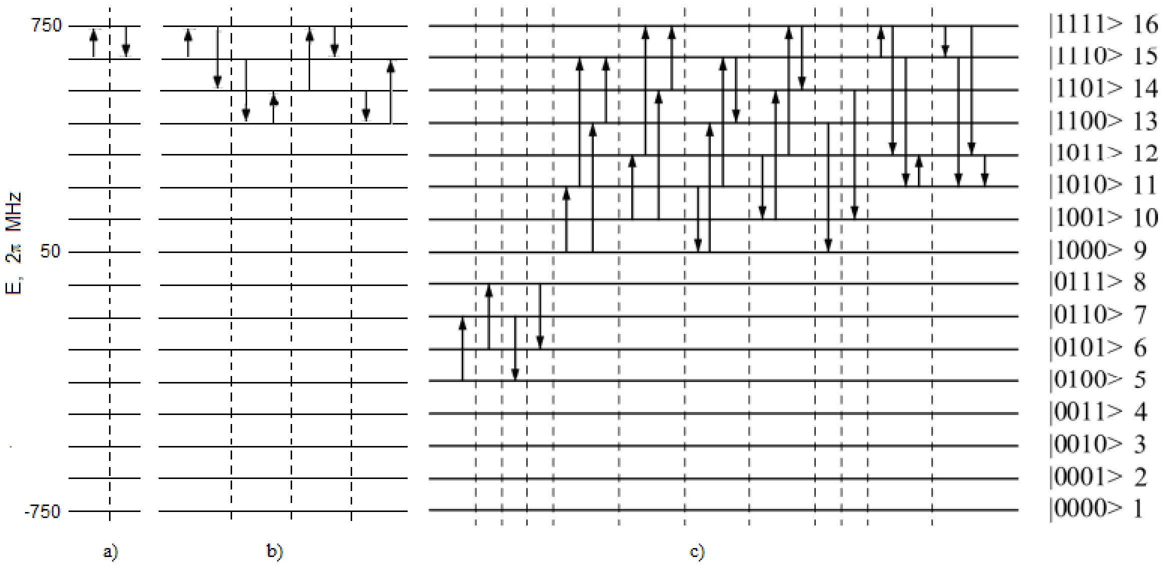

Fig. 2. Energy levels and allowed transitions for the four-qubit Toffoli (a), Fredkin (b) and Peres gates (c).

Let us consider examples of the allowed transitions in the four-qubit gates.

1) The allowed transitions for the four-qubit Toffoli gate (Fig. 2a) are:

$15|1110\rangle \to 16|1111\rangle$ and $16|1111\rangle \to 15|1110\rangle$,

where the last (target) qubit changes its state at the output according to (1). The decimal notation for the states adopted in the article is shown in Fig. 2.

2) The four-qubit Fredkin gate can be implemented in this model with only two transitions, namely (Fig. 2b):

$15|1110\rangle \to 14|1101\rangle$ and $14|1101\rangle \to 15|1110\rangle$.

However, according to the Pauli exclusion principle, these transitions are forbidden, so their implementation is possible through some intermediate levels. The following two-step transitions implemented under action of two π-pulses (duration π/Ω) are permitted when tuning the RF control magnetic field into the resonance:

$$15|1110\rangle \to 16|1111\rangle \to 14|1101\rangle,$$

$$15|1110\rangle \to 13|1100\rangle \to 14|1101\rangle,$$

and

$$14|1101\rangle \to 16|1111\rangle \to 15|1110\rangle,$$

$$14|1101\rangle \to 13|1100\rangle \to 15|1110\rangle.$$

In this case, when the first two (control) qubits are set to state 1, the last two (target) qubits exchange their values according to (2). Increasing the number of control qubits does not change the number of π-pulses that provide algorithmic gate transitions, since in the one and two-stage transitions, only target qubits change, while the control qubits remain unchanged. This effect is also valid for the multiple-control Toffoli gate.

3) Allowed transitions that implement the four-qubit Peres gate according to (3) are presented in Fig. 2c [14]:

$$5|0100\rangle \to 7|0110\rangle,\ \ 6|0101\rangle \to 8|0111\rangle,$$

$$7|0110\rangle \to 5|0100\rangle,\ \ 8|0111\rangle \to 6|0101\rangle,$$

$$13|1100\rangle \to 9|1000\rangle,\ \ 14|1101\rangle \to 10|1001\rangle.$$

For simplicity, we use both decimal and binary notations. Forbidden transitions $9 \to 15$, $10 \to 16$, $11 \to 13$, $12 \to 14$, $15 \to 12$, and $16 \to 11$ can be implemented in two steps. For example, the forbidden transition $9 \to 15$ can be implemented in two different ways:

$12|1011\rangle \to 16|1111\rangle \to 14|1101\rangle$ and

$12|1011\rangle \to 10|1001\rangle \to 14|1101\rangle$.

For allowed transitions, the frequency of the radio-frequency field is defined by the energy of the transition

$$\omega_{mn} = \frac{E_m - E_n}{\hbar}. \qquad (8)$$

Along with pure digital states, the quantum gates also implement transitions between superposition states. In further calculations, as the digital states we mean pure (not superposition) states. At the same time, we carried out the analysis of superposition states using an equally probable superposition as an example. However, both the former and latter ones are negatively affected by the frequency noise, which is caused by an inaccurate tuning the radio-frequency pulse generator in frequency and also in phase. These factors will inevitably affect the gate fidelity. In particular, the fidelity value in optical systems of about 68% for the Fredkin gate and 81% for Toffoli gate has been recently observed experimentally [5].

4. Results and discussion

We can quantitatively describe the correctness of the gates quantum algorithm using the fidelity [14]:

$$F = \langle \Psi(t) | \Psi_0(t) \rangle. \qquad (9)$$

Here, $\Psi(t)$ and $\Psi_0(t)$ are the proper wave functions obtained from the solution of the equation (7) at the frequencies ω and ω_{mn}, respectively. In our interpretation, the value $|F|^2$ is the probability of correct operation of the gate.

The Larmor frequencies ($\omega_k = \gamma B(x_k)$), as well as the Rabi frequencies ($\Omega = \gamma b$), depend on the external magnetic field (static $B(x_k)$ and transverse radio-frequency b, respectively). In an ideal model, their amplitudes are considered as a constant throughout the control pulse. However, under the influence of environment and due to inaccuracies in tuning the RF pulse generator the variations of these frequencies take place, leading to the so-called frequency noise. The latter leads to an imbalance of the system and, as a consequence, to incorrect operation of the studied quantum gates.

Firstly, let us consider the negative effect of frequency noise on correct operation of the multiple-control gates, depending on the number of control signals. This noise may be caused by the inaccuracy in tuning the frequency ω of the RF generator, which is different from the resonant frequency ω_{mn} of the transition:

$$\omega = \omega_{mn}(1 + \eta), \qquad (10)$$

where η is the frequency imbalance parameter. In Fig. 3, we present the fidelity as a function of the parameter η for the four-qubit Toffoli ($15 \to 16$), Fredkin ($15 \to 16 \to 14$), and Peres ($12 \to 16 \to 14$) gates.

For the digital states, the fidelity decreases sharply with increasing η (Fig. 3b), with the maximum imbalance corresponding to $F = 0.9$, which is independent

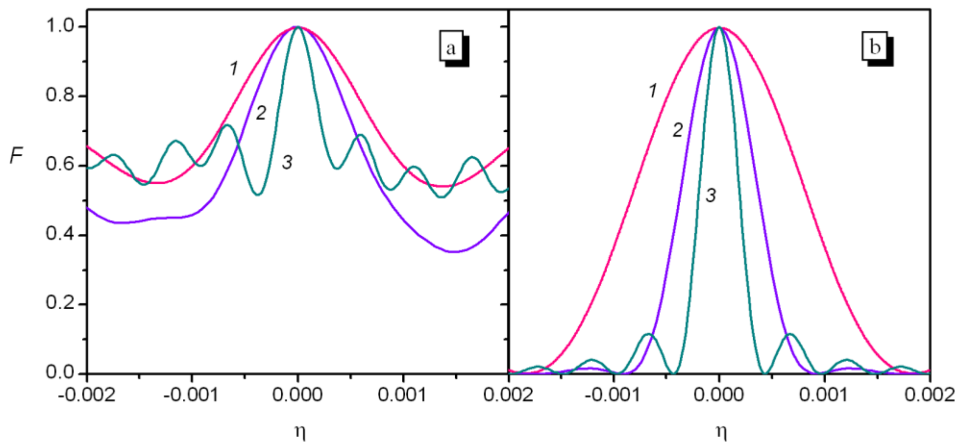

Fig. 3. Fidelity as a function of the relative error η for the four-qubit gates: *1* – Toffoli (15→16), *2* – Fredkin (15→16→14) and *3* – Peres (12→16→14) gates. a) superposition states; b) digital states.

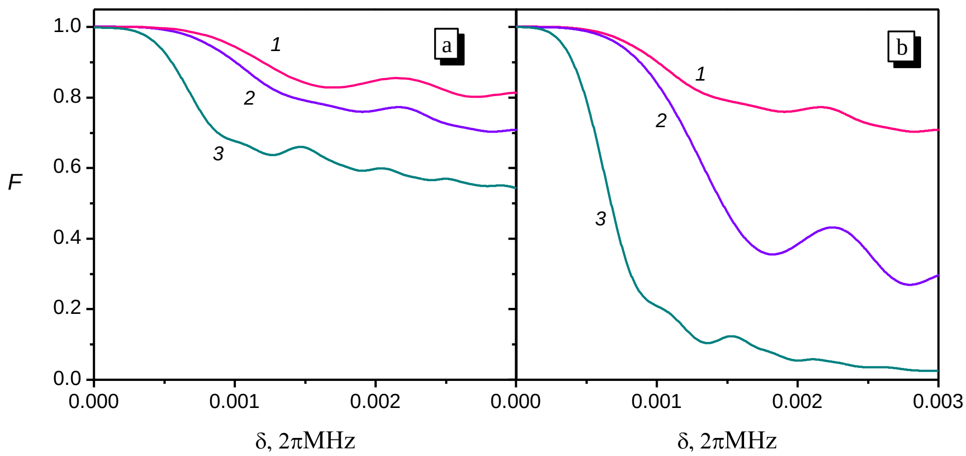

Fig. 4. Fidelity as a function of the parameter δ for the four-qubit gates: *1* – Toffoli (15 → 16), *2* – Fredkin (15 → 16 → 14) and *3* – Peres (15 → 16 →12) gates; a) superposition states; b) digital states.

of both the number of the control qubits of the Toffoli and Fredkin gates and the type of transition (see Table). At the same time, the dependence $F(\eta)$ decreases with increasing the number of the control qubits for the generalized Peres gate, which can be explained by its more complex logical structure. The calculation for the uniformly filled superposition states with the probability 1/16 gives a much more complicated dependence $F(\eta)$ (Fig. 3a). In particular, the maximum value of the parameter η, which corresponds to the correct operation ($F = 0.9$) of the gates, significantly increases and depends on the type of the algorithmic transition.

As the number of qubits N increases, the situation for the superposition states is the same as in the case of the digital states, that is, the fidelity remains constant for the Toffoli and Fredkin gates, and decreases for the Peres gates (Table). These results may be related to the different maximal values of transition energies for the gates under consideration. For example, the maximal energies of the transition in the four-qubit gates are: 95.5 2π·MHz for the 15 → 16 transition in the Toffoli gate, 189.5 2π·MHz for the 15 → 16 → 14 transitions in the Fredkin gate and 389.5 2π·MHz for the 12 → 16 → 14 transition in the Peres gate. The higher these energies, the more sensitive is the gate to the frequency noise. This is also true with the increase of the number of qubits N, since the maximal transition energies are increased only in the Peres gate with increasing N.

Another type of frequency noise is small periodic frequency oscillations over time that can be described as

$$\omega = \omega_{mn} \cos(\delta t), \qquad (11)$$

where the parameter δ characterizes time deviation of the frequency of the RF generator relative to the resonant frequency of the transition that implements the Toffoli, Fredkin, and Peres gates. Analysis of the fidelity dependences for this type of noise on the imbalance parameters makes it possible to state that, as in the previous case for

Table. Frequency imbalance parameter η (relative units) and modulation imbalance parameter δ (in 2π MHz) for the *N*-qubit gates (*N* = 3, 4, 5, 6, 7).

N	Digital states						Superposition states					
	Toffoli gate		Fredkin gate		Peres gate		Toffoli gate		Fredkin gate		Peres gate	
	η, 10^{-4}	δ, 10^{-4}	η, 10^{-4}	δ, 10^{-4}	η, 10^{-4}	δ, 10^{-4}	η, 10^{-4}	δ, 10^{-4}	η,10^{-4}	δ, 10^{-4}	η, 10^{-4}	δ, 10^{-4}
3	6.82	8.84	2.63	5.68	1.4	2.22	7.61	12.1	3.52	3.87	2.62	3.22
4	6.82	8.84	2.65	1.33	0.72	1.54	7.61	12.1	3.54	1.79	0.32	2.16
5	6.82	8.84	2.57	0.68	0.34	0.65	7.61	12.1	3.48	0.75	0.15	0.88
6	6.82	8.84	2.55	0.12	0.13	0.09	7.61	12.1	3.47	0.56	0.09	0.37
7	6.82	8.84	2.51	0.05	0.04	0.01	7.61	12.1	3.41	0.49	0.02	0.12

the digital states, $F(\delta)$ decreases rather sharply with increasing the parameter δ (Fig. 4b) and does not depend on the type of transition. For the superposition states, an increase in the possible values of the parameter δ for correct operation ($F \geq 0.9$) was found (Table).

As follows from this table, an increase in the number of control qubits for the generalized Toffoli gate does not affect the value of its fidelity. However, the $F(\delta)$ dependences for Fredkin and Perez gates show a decrease depending on the frequency imbalance parameter δ of the RF control field. It should be noted that, regardless of the noise type, the correctness of multiple-control Toffoli and Fredkin gates operation remains unchanged for the digital states with increasing *N*. At the same time, frequency noise leads to destruction of the superposition states in the generalized Fredkin and Peres gates.

The results can be generalized to the case of the multiple-control gates with an arbitrary number of qubits. For the Toffoli and Fredkin gates, an increase in the number of control qubits does not affect the structure of the allowed transitions and results only in renumbering the system energy levels (Figs 2a, 2b). At the same time, an increase in *N* for the Peres gate leads to a more complicate structure of the allowed transitions (Fig. 2c), in accordance with the algorithm (3).

To take into account an inaccuracy in tuning the frequency of the RF generator, it is necessary to choose the optimal values of the imbalance parameters. In Fig. 5, we present the dependences of the imbalance parameter η on the dimensionless parameter ω_0/J, which allows us to choose the best values of both the magnitude of the magnetic field and the parameter of the exchange interaction. The choice of the latter is defined by the physical properties of the impurity atom (qubit), the distance between qubits, *etc.* [16]. In particular, for correct operation of the four-qubit Fredkin gate on pure digital states, the imbalance parameter $\eta = 2.65 \cdot 10^{-4}$ corresponds to $\omega_0/J = 20$, while for the superposition states $\eta = 3.54 \cdot 10^{-4}$ corresponds to $\omega_0/J = 8$. The value of ω_0/J obtained for the four-qubit gate agrees with the estimate [5], where it is ~23. Presented in Fig. 5 dependences also allow finding the optimal ratio ω_0/J for the Toffoli gate – 16 ([5]) and for the Peres gate – 12.

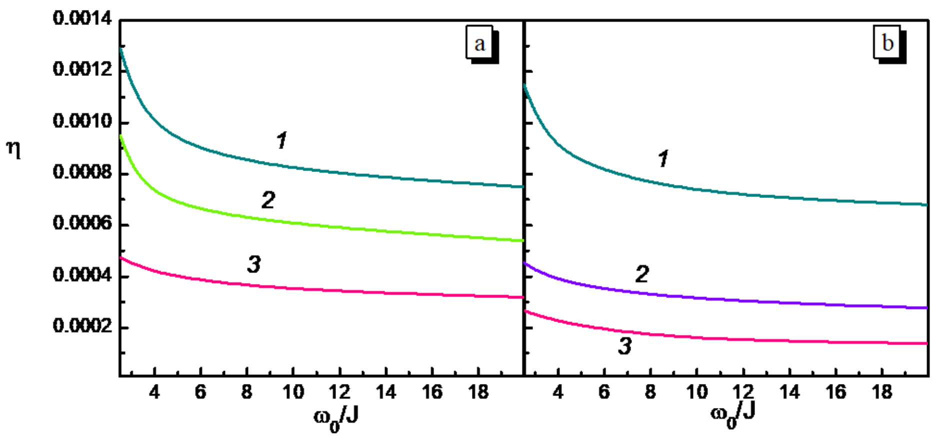

Fig. 5. Dependence of the imbalance parameter η on the ratio ω_0/J for the four-qubit gates: *1* – Toffoli (15 → 16 transition), *2* – Fredkin (15 → 16 → 14 transition) and *3* – Peres (12 → 16 → 14 transition) gates. a) superposition states; b) digital states.

5. Conclusions

In the paper, we have presented the design of the multiple-control Toffoli, Fredkin and Peres gates in the model of a nuclear spin chain in a spinless semiconductor matrix. The comparison of the number of required transitions, which realizes correct operation of the gates, with the number of control qubits has been performed. The allowed transitions that realize gates operation for one and two π-pulses have been determined. The analysis of the fidelity as a characteristic of system correct operation has carried been out. It has been shown that for the multiple-control Toffoli and Fredkin gates, the fidelity does not depend on the number of control qubits for different types of the frequency noise caused by an imbalance of the RF control field generator. At the same time, for the multiple-control Peres gate, the fidelity is quite sensitive to the number of control qubits and decreases sharply with increasing the number of these qubits. From the foregoing, it follows that the multiple-control Toffoli and Fredkin gates are more suitable for practical use, since they are less affected by the frequency noise than the Peres gates. Comparison of the fidelities for the digital and superposition states allows us to make an unexpected conclusion about the higher stability of the latter, which is typical for all the gates under study. The calculated values of the parameter ω_0 / J give the possibility to make the optimal choice of the external constant magnetic field and the parameter of the exchange interaction between qubits. The obtained results can be used in the design of the quantum semiconductor NMR processors.

References

1. Nielsen M.A., Chuang I.L. *Quantum Computation and Quantum Information*. Cambridge: Cambridge University Press, 2000.
2. Bérut A., Petrosyan A., Ciliberto S. Information and thermodynamics: Experimental verification of Landauer's erasure principle. *Journal of Statistical Mechanics: Theory and Experiment*. 2015. **2015**, No 6. P06015. https://doi.org/10.1088/1742-5468/2015/06/P06015.
3. IBM QX backend information (2018). Available at https://github.com/QISKit/ibmqx-backend-information.
4. Morello A., Tosi G., Mohiyaddin F.A. *et al.* Scalable quantum computing with ion-implanted dopant atoms in silicon. *IEEE International Electron Devices Meeting*. 2018. P. 6.2.1–6.2.4. San Francisco, CA. https://doi.org/10.1109/IEDM.2018.8614498.
5. Stojanović V.M. Feasibility of single-shot realizations of conditional three-qubit gates in exchange-coupled qubit arrays with local control. *Phys. Rev. A*. 2019. **99**, No 1. P. 012345. https://doi.org/10.1103/PhysRevA.99.012345.
6. Maslov D., Dueck G., Miller D. Synthesis of Fredkin-Toffoli reversible networks. *IEEE Transactions on VLSI Systems*. 2005. **13**, No 6. P. 765–769. https://doi.org/10.1109/TVLSI.2005.844284.
7. Saeedi M. and Markov I.L. Synthesis and optimization of reversible circuits – a survey. *ACM Comput. Surv*. 2013. **45**, No 2. Article 21. https://doi.org/10.1145/2431211.2431220.
8. Donald J., Jha N.K. Reversible logic synthesis with Fredkin and Peres gates. *J. Emerg. Technol. Comput. Syst*. 2008. **4**, No 1. Article 2. https://doi.org/10.1145/1330521.1330523.
9. Picton P.D. Modified Fredkin gates in logic design. *Microelectron. J*. 1994. **25**, No 6. P. 437–441.
10. Szyprowski M., Kerntopf P. Low quantum cost realization of generalized Peres and Toffoli gates with multiple-control signals. *Proc. 13th IEEE Conference on Nanotechnology*, Beijing, China, 5-8 Aug. 2013. P. 802–807. https://doi.org/10.1109/NANO.2013.6721034.
11. Pla J.J., Tan K.Y., Dehollain J.P. *et al*. High-fidelity readout and control of a nuclear spin qubit in silicon. *Nature*. 2013. **496**(7445). P. 334–338. https://doi.org/10.1038/nature12011.
12. Zhang X., Li H., Cao G., Xiao M., Guo G. Semiconductor quantum computation. *National Science Review*. 2019. **6**, No 1. P. 32–54. https://doi.org/10.1093/nsr/nwy153.
13. Xue F., Du J.-F., Shi M.-J. *et al*. Realization of the Fredkin gate by three transition pulses in a nuclear magnetic resonance quantum information processor. *Chin. Phys. Lett*. 2002. **19**, No 8. P. 1048–1050.
14. Rozhdov O., Yuriychuk I., and Deibuk V. Building a generalized Peres gate with multiple control signals. *Advances in Intelligent Systems and Computing*. 2019. **754**. P. 155–164. https://doi.org/10.1007/978-3-319-91008-6_16.
15. Yuriychuk I., Hu Z., and Deibuk V. Effect of the noise on generalized Peres gate operation. *Advances in Intelligent Systems and Computing*. 2020. **938**. P. 428–437. https://doi.org/10.1007/978-3-030-16621-2_40.

Authors and CV

V.G. Deibuk, Professor, Doctor of Sciences in Physics and Mathematics, Professor of Computer Systems and Networks Department at the Yuriy Fedkovych Chernivtsi National University. The area of his scientific interests includes computer simulation of physical properties of semiconductors, quantum and reversible computing, artificial intelligent methods.

I.M. Yuriychuk, PhD in Physics and Mathematics, Associate Professor, Senior Researcher of Department of Electronics and Energy at the Yuriy Fedkovych Chernivtsi National University. The area of his scientific interests includes physics of nanoscale semiconductor structures and quantum computing.

I. Lemberski, Professor, Doctor of Sciences in Physics and Mathematics, Senior Researcher at the Ventspils University College, International Radio Astronomy Centre, Latvia. His research interests include all aspects of discrete circuits logic synthesis and reversible computing.

Чіткість спрацювання зашумлених багатоконтрольованих зворотних логічних елементів

В.Г. Дейбук, І.М. Юрійчук, І. Лемберскі

Анотація. Вивчено вплив частотного шуму на коректну роботу багатоконтрольованих зворотних елементів Тоффолі, Фредкіна та Переса. У рамках моделі Ізінга отримано енергетичний спектр ланцюжка атомів з ядерними спінами ½ у безспіновій напівпровідниковій матриці та визначено допустимі переходи, що відповідають алгоритму роботи цих логічних елементів. Вірність спрацювання отриманих переходів вивчено в залежності від кількості контрольних кубітів та параметрів радіочастотних керуючих імпульсів. Показано, що правильна робота зворотних елементів Тоффолі та Фредкіна не залежить від кількості контролюючих кубітів, тоді як вірність спрацювання елементів Переса значно зменшується зі збільшенням кількості керуючих сигналів. Розраховане відношення частоти Лармора до постійної обмінної взаємодії добре узгоджується з результатам інших досліджень.

Ключові слова: квантові обчислення, багатоконтрольованість, елемент Фредкіна, елемент Тоффолі, елемент Переса, чіткість спрацювання.